Identification of the critical temperature from non-equilibrium time-dependent quantities

Identification of the critical temperature from non-equilibrium time-dependent quantities

E. LIPPIELLO[1(a)] and A. SARRACINO[2,3]

[1] *Dipartimento di Scienze Ambientali and CNISM, Seconda Università di Napoli - Via Vivaldi, 81100 Caserta (CE), Italy, EU*
[2] *Dipartimento di Matematica ed Informatica, Università di Salerno - Via Ponte don Melillo, 84084 Fisciano (SA), Italy, EU*
[3] *CNR - ISC and Dipartimento di Fisica, Università Sapienza - p.le A. Moro 2, 00185 Roma, Italy, EU*

Abstract – We present a new procedure that can identify and measure the critical temperature. This method is based on the divergence of the relaxation time approaching the critical point in quenches from infinite temperature. We introduce a dimensionless quantity that turns out to be time independent at the critical temperature. The procedure does not need equilibration and allows for a relatively fast identification of the critical temperature. The method is first tested in the ferromagnetic Ising model and in the two-dimensional EA model and then applied to the one-dimensional Ising spin glass with power law interactions. Here we always find a finite critical temperature also in the presence of a uniform external field, in agreement with the mean-field picture for the low-temperature phase of spin glasses.

The identification of a critical temperature T_c is a fundamental characterization of statistical systems. This, indeed, allows one to construct the phase diagram of the system and to obtain insights in the underlying relevant physical mechanisms. In many cases the existence/absence of a phase transition discriminates among different pictures for a given system. A major example is the long-standing question on the nature of the spin glass phase in finite-dimensional systems. According to the replica symmetry breaking scenario [1], a transition line should exist, the so-called de Almeida-Thouless (AT) line, separating the paramagnetic from the spin glass phase in the temperature *vs.* magnetic field phase diagram [1,2]. More precisely, the spin glass phase is not destroyed by applying an external field. Conversely, other theories, as the "droplet picture" [3], predict no AT line. Therefore, the identification of a critical temperature in the presence of an external perturbation discriminates between the different theories.

The critical point is usually identified with the temperature $T = T_c$ where the equilibrium correlation length $\xi(T)$

diverges. This property reflects on the behavior of the order parameter correlation function $C(r)$ whose asymptotic decay changes from exponential to algebraic when approaching T_c. Such a study is often hindered by the fact that also the relaxation time t_{eq} diverges for temperatures close to T_c and it is only possible to equilibrate systems of small size L. However, it is possible to extrapolate the critical temperature in the $L \to \infty$ thermodynamic limit from the behavior of finite systems by means of well-established methods such as Finite Size Scaling (FSS) [4]. The most used method for the identification of T_c, generally known as Phenomenological Renormalization, consists in the introduction of an appropriate dimensionless quantity that is expected to cross exactly at the critical point [5]. In the specific case of magnetic systems, one usually measures [6–9] a finite-size correlation length $\xi(L,T)$ at the temperature T, as for instance $\xi(L,T)^2 = (\int_0^L \mathrm{d}r\, r^2 C(r,T))/\int_0^L \mathrm{d}r\, C(r,T)$ [10]. The dimensionless quantity $X(L,T) = \xi(L,T)/L$ is then plotted over T for different values of L. According to FSS, one expects the following relation:

$$X(L,T) = f\left[\xi(T)/L\right], \tag{1}$$

⎯⎯⎯⎯⎯⎯⎯⎯⎯⎯
[(a)]E-mail: lippiello@sa.infn.it

implying that $X(L,T)$ becomes L independent when $\xi(T)$ diverges, namely for $T = T_c$. T_c is therefore given by the temperature where curves for different L intersect.

On the other hand, one can identify T_c exploiting the intrinsically non-equilibrium nature of the critical point as, for instance, implemented in Short-Time Dynamics (STD) [11], Non-Equilibrium Relaxation (NER) [12] or other methods which use both equilibrium and non-equilibrium measurements [13]. These are substantially based on the dynamical scaling hypothesis assuming the existence at the time t of a typical dynamic length $L(t)$. The divergence of the relaxation time at T_c then reflects on a power law temporal decay of some observables such as the magnetization.

In this letter, exploiting dynamical scaling as in NER methods, we propose a procedure to identify T_c that uses phenomenological renormalization techniques with non-equilibrium time-dependent quantities. More precisely, we set $L \to \infty$ from the beginning, and replace in eq. (1) space distances with times introducing the dimensionless quantity

$$X(\tau,T) = \frac{1}{\tau} \frac{\int_0^\tau \mathrm{d}t \, t C(t,T)}{\int_0^\tau \mathrm{d}t C(t,T)}, \qquad (2)$$

where t is the time since the quench at the temperature T from a disordered initial condition, τ is a fixed time and $C(t,T)$ is the correlation function with the initial configuration. For instance, for spin systems, $C(t,T) = \langle (s_i(t) - \langle s_i(t) \rangle)(s_i(0) - \langle s_i(0) \rangle) \rangle$, with $s_i(t)$ the spin in the position i at time t. The average is performed over initial conditions, non-equilibrium dynamics at the temperature T, and quenched disorder if present. We always take initial conditions corresponding to equilibrium at infinite temperature, and therefore $\langle s_i(0) \rangle = 0$ and $C(t,T) = \langle s_i(t)s_i(0) \rangle$. Let us notice that other quantities can be equivalently considered in the definition of $X(\tau,T)$. Here we use the two-time correlation function, that is more easily obtained in numerical simulations. However one can also use the thermo-remanent magnetization, more suitable in experimental settings. Dynamical scaling, then, predicts

$$X(\tau,T) = g[t_{eq}(T)/\tau], \qquad (3)$$

where $t_{eq}(T)$ is the relaxation time for quenches at the temperature T. The divergence of $t_{eq}(T)$ approaching T_c implies that $X(\tau,T)$ does not depend on τ when $T = T_c$. Therefore, considering different values of τ and plotting $X(\tau,T)$ *vs.* T, one identifies T_c as the intersection point of the different curves.

The above procedure does not require to equilibrate the system, leading to some advantages with respect to the FSS method. Indeed, in experiments, the sample sizes always fulfill the thermodynamic limit and one cannot explore the L-dependence. Conversely, one can measure $X(\tau,T)$ for different time interval τ and different T. From a numerical point of view, in particular for spin glasses, the equilibration of the system is numerically hard to achieve and to check. Indeed, equilibration is very

time-demanding and indirect checks are always necessary in order to verify that a true equilibrium state is attained. Moreover, in our approach, by means of a single simulation up to the final time t_f, one can compute $X(\tau,T)$ for many values of $\tau \in [0,t_f]$. Conversely, in the FSS method one has just one $X(L,T)$ for each simulation with a system of size L. Another difference relies on the possibility of using simple spin-spin correlations as $C(t,T)$ also in disordered systems, where, generally, the identification of a correlation length necessitates the computation of multispin correlation functions [14]. The presence of disorder, indeed, makes $\xi(L,T)$ invisible to equal time spin-spin correlation function. Conversely, $C(t,T)$ is strongly affected by $t_{eq}(T)$. A final remark concerns the possibility to better control the influence of scaling corrections in the estimated T_c. Indeed, a pure power law decay $C(t,T) \sim t^{-\theta_c}$ must be observed at $T = T_c$, leading to $X(\tau,T_c) = (1 - \theta_c)/(2 - \theta_c)$. The exponent θ is related to the Fisher-Huse exponent λ via the relation $\theta = \lambda/z$, where z is the growth exponent.

The measured X at the intersection point, therefore, gives an estimate for θ_c and corrections to scaling should be observed as deviations from this power law decay of $C(t,T)$. Let us notice, however, that a precise measurement of T_c can be only obtained for very large τ. From dynamical scaling, evolution up to a finite time t_f corresponds to equilibration up to a size $L(t_f)$, and the accuracy in the determination of T_c is then of the same order of FSS analysis on system up to size $L(t_f)$. In the following we present results involving not very large simulation times ($\sim 12\,\mathrm{h}$ of cpu time for each temperature), that, however, are sufficient to identify the critical temperature with a reasonable accuracy. For each given system and each temperature we consider about 1000 independent realizations.

Dynamical evolution is obtained via standard Monte Carlo simulations and $X(T,\tau)$ is obtained after the integration of $C(t,T)$ with a time-step of single spin update. In all cases we always take different sample sizes L in order to check that no finite-size effects are present.

Let us begin by checking our method in cases where the critical temperature is well known. In particular, we start by considering the Ising model with Hamiltonian $\mathcal{H} = -\sum_{\langle ij \rangle} J_{ij} s_i s_j$ and ferromagnetic coupling $J_{ij} = J$ in two and three dimensions. In these cases $T_c \simeq 2.269J$ and $T_c \simeq 4.5115J$ are, respectively, analytically and numerically known [15]. In the following we always take $J = 1$ for simplicity. The behavior of $C(t,T)$ can be obtained from general arguments [11,16,17], giving $C(t,T) \sim t^{-\theta_c} e^{-t/t_{eq}(T)}$ for $T \gtrsim T_c$, where θ_c can be related to static and dynamic critical exponents, and $C(t,T) \sim t^{-\theta}$ with $\theta < \theta_c$ for $T < T_c$. Then one has, for large τ and $\theta_c < 1$

$$X(\tau,T) \to \begin{cases} t_{eq}(T)/\tau, & \text{for} \quad T \gtrsim T_c, \\ (1 - \theta_c)/(2 - \theta_c), & \text{for} \quad T = T_c, \\ X_0 = (1 - \theta)/(2 - \theta), & \text{for} \quad T < T_c. \end{cases} \qquad (4)$$

Fig. 2: (Color online) $X(\tau, T)$ vs. T for different values of τ for the EA model in $d = 2$. In the inset $T_c(\tau_i)$ is plotted vs. τ_i supporting the absence of a finite T_c.
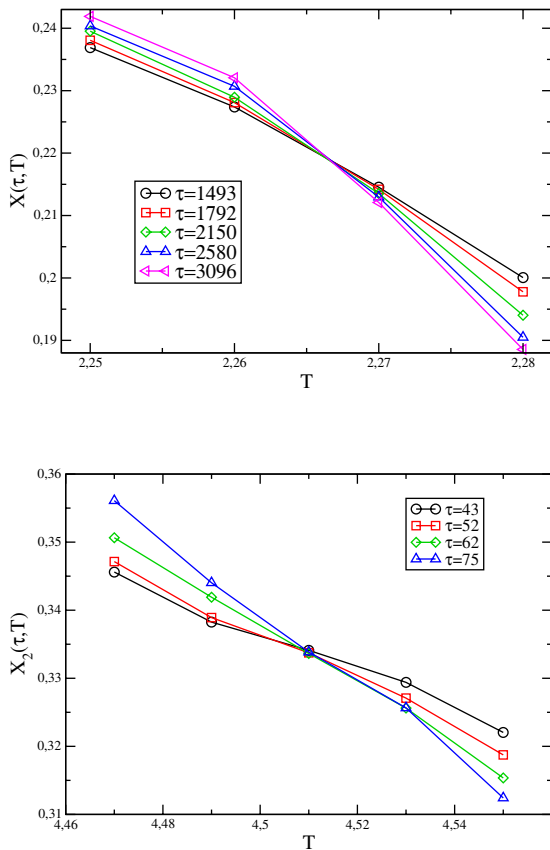

Fig. 1: (Color online) $X(\tau, T)$ and $X_2(\tau, T)$ are plotted vs. T for different values of τ for the Ising model in $d = 2$ and $d = 3$, respectively. Data cross around the known critical temperatures $T_c = 2.269$ and $T_c = 4.511$. In $d = 2$, $\theta \sim 0.625$ for $T < T_c$ and $\theta_c \sim 0.74$, while in $d = 3$, $\theta \sim 1.3$ for $T < T_c$ and $\theta_c \sim 1.4$. In the inset of the upper panel the quantity $X(\tau, T)$ is plotted over τ for different temperatures. In the numerical simulations we consider systems of $N = L^d$ spins, with $L = 400$ for $d = 2$ and $L = 128$ for $d = 3$.

More precisely, for $T < T_c$, the dynamics is initially attracted by the critical point at T_c [18] and then converges, for large τ, to $X_0 > X(\tau, T_c)$. This implies that $X(\tau, t)$ diminishes by increasing τ for $T > T_c$, grows until it converges to X_0 when $T < T_c$, and is τ independent at T_c. In the upper panel of fig. 1 the quantity $X(\tau, T)$ is plotted over the temperature for different values of τ, for the two-dimensional Ising model evolving via Glauber dynamics. One clearly observes that the curves intersect in a narrow region giving $T_c = 2.268 \pm 0.002$ in agreement with the analytical result.

In the case of $d = 3$, since $\theta_c \sim 1.4 > 1$ [19], the integral $\int_0^\tau dt\, t^{-\theta_c}$ diverges, making $X(\tau, T)$ useless for extracting critical behaviors. One then can overcome this problem considering the "second moment" $X_2(\tau, T) = \frac{1}{\tau} \frac{\int_0^\tau dt\, t^2 C(t,T)}{\int_0^\tau dt\, t C(t,T)}$, that is expected to converge to $(2 - \theta_c)/(3 - \theta_c)$ for the critical quench. In the lower panel of fig. 1 the quantity $X_2(\tau, T)$ is plotted vs. the temperature for different values of τ. One again clearly
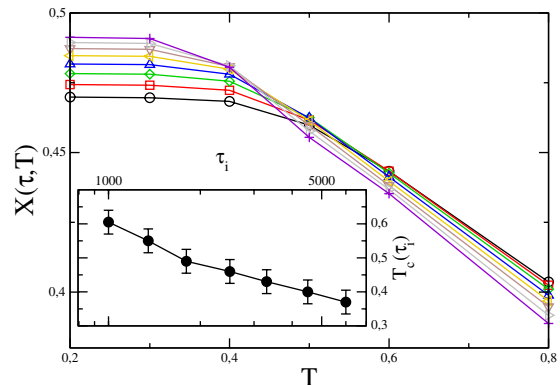
observes that the curves intersect in a narrow region giving $T_c = 4.510 \pm 0.003$, in agreement with previous numerical results.

As intermediate case between ferromagnets and spin glass systems, we have also considered the diluted Ising model. In this model the spin coupling J_{ij} is chosen to be J with probability p and to be 0 with probability $1 - p$. Our results substantially agree with previous accurate estimates of T_c in ref. [7], for different choices of the parameter p. As a further test, we have considered the $d = 2$ Edwards-Anderson model, where previous studies clearly indicate the absence of a phase transition at finite temperature [20–22]. More precisely, we have investigated systems with $N = 400^2$ spins and bimodal couplings $J_{ij} = \pm 1$ with equal probability. Results, plotted in fig. 2, show that curves corresponding to different τ do not intersect in the same point but the intersection points move towards the left by increasing τ. More precisely, in the inset of fig. 2, we plot the "critical temperature" $T_c(\tau_i)$ identified from the intersection between the curves for $X(\tau_i, T)$ and $X(\tau_{i+1}, T)$. We chose $\tau_{i+1} = \alpha \tau_i$ with $\tau_1 = 1000$ and $\alpha = 1.35$. The inset clearly shows that $T_c(\tau_i)$ decreases for increasing τ_i, indicating an asymptotic convergence $T_i \to 0$ at large times. This result supports the absence of a finite critical temperature. The same analysis performed for the other cases where a finite T_c has been identified, gives a $T_c(\tau_i)$ fluctuating around T_c.

Next we consider the case of the one-dimensional Ising spin glass with power law decaying interactions [23]. The system is defined by the Hamiltonian $\mathcal{H} = -\sum_{i,j} J_{ij} s_i s_j - h \sum_i s_i$, where the site i belongs to a ring of length L and h is a magnetic field. The sum is over all spins of the ring and $J_{ij} = c(\sigma) \epsilon_{ij} / r_{ij}^\sigma$, where ϵ_{ij} are chosen according to a Gaussian distribution with zero mean and standard deviation unity. The constant $c(\sigma)$ is chosen to give a mean-field transition temperature $T_c^{MF} = 1$, namely

$$1 = (T_c^{MF})^2 = \sum_{j \neq i} [J_{ij}^2]_{av} = c(\sigma) \sum_{j \neq i} \frac{1}{r_{ij}^{2\sigma}}, \quad (5)$$
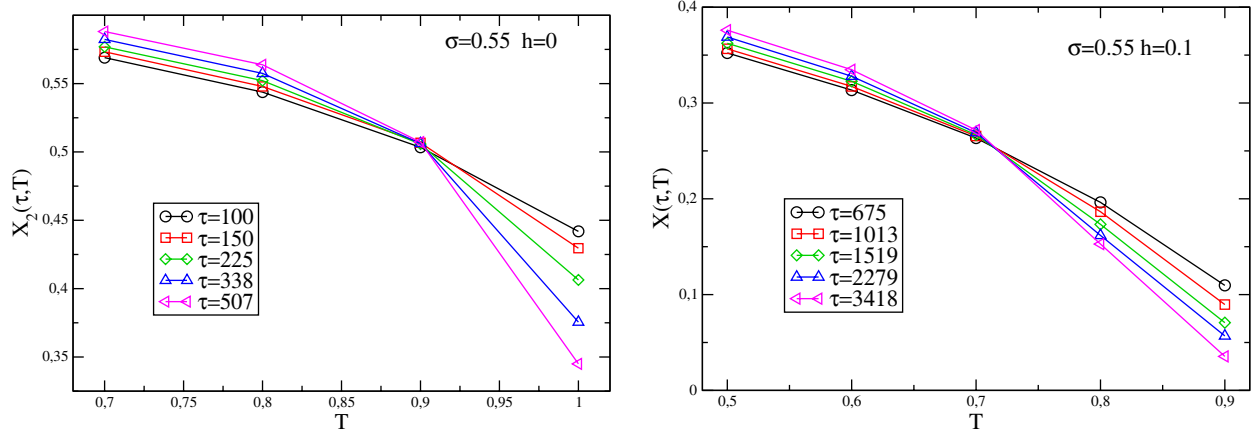
Fig. 3: (Color online) The quantities $X_2(\tau, T)$ and $X(\tau, T)$ are plotted *vs.* the temperature for different values of τ, in the one-dimensional Ising spin glass with power law interactions, for $\sigma = 0.55$ and $h = 0, 0.1$. In all cases the curves cross, indicating the presence of a finite critical temperature.
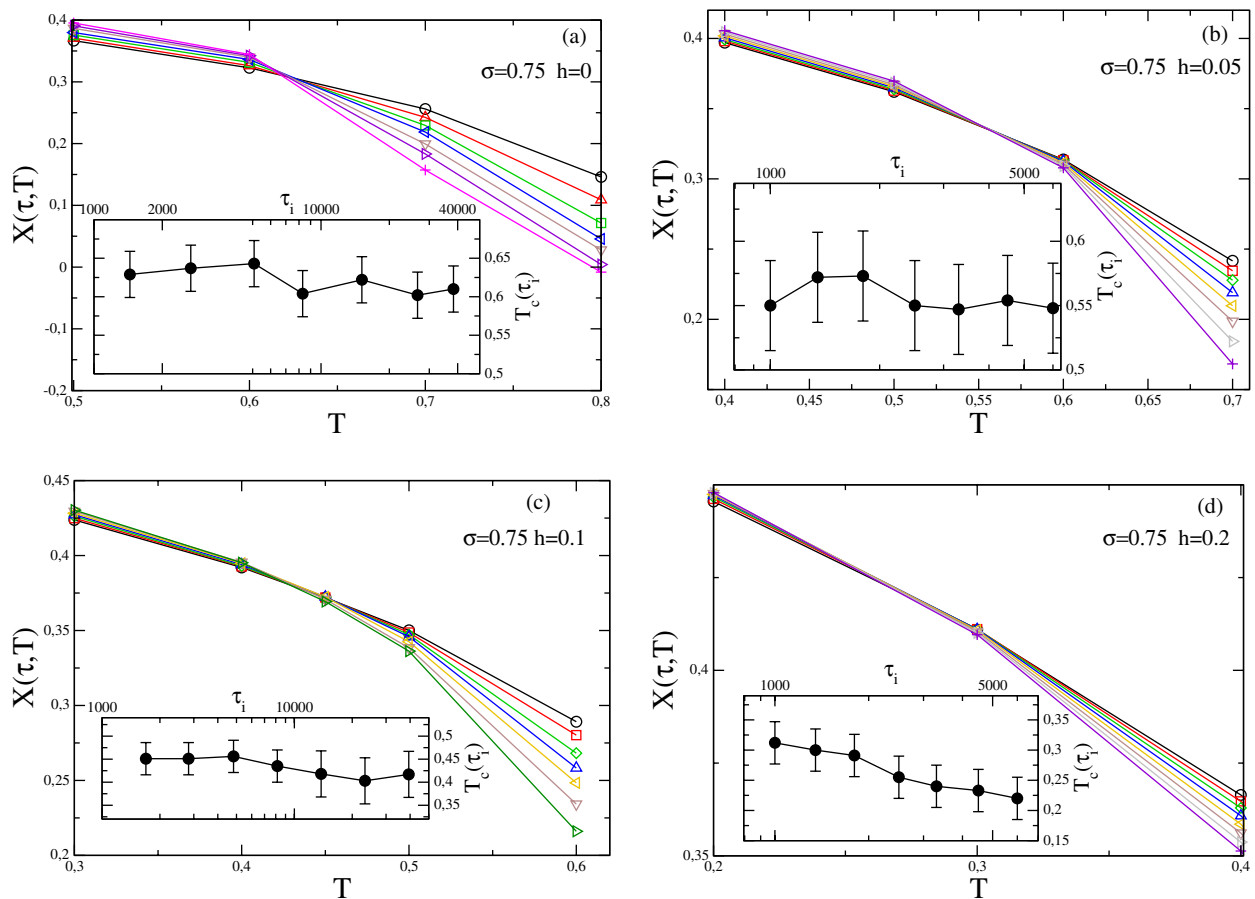

Fig. 4: (Color online) The quantities $X(\tau, T)$ is plotted over the temperature in the one-dimensional Ising spin glass with power law interactions, for $\sigma = 0.55$ and $h = 0, 0.05, 0.1, 0.2$. Curves correspond to different τ_i obtained by the relation $\tau_{i+1} = 1.35\tau_i$ and $\tau_1 = 1000$. In the insets the plot $T_c(\tau_i)$ *vs.* τ_i gives a finite critical temperature for $h = 0, 0.05, 0.1$ and suggests $T_c = 0$ for $h = 0.2$.

where $[\dots]_{av}$ denotes an average over disorder. The distance between two spins on the ring in terms of L is $r_{ij} = (L/\pi) \sin(\pi |i - j| / L)$. By varying the strength of the interaction through the parameter σ, this model shows different behaviors [23]. In particular, for $\sigma = 0$, taking

$c(\sigma) \sim 1/\sqrt{N}$, one recovers the Sherrington-Kirkpatrick model [24]. For $\sigma \in [1/2, 1]$ the system shows a finite critical temperature, with a mean-field–like region for $\sigma \in [1/2, 2/3]$ and a non–mean-field region for $\sigma \in (2/3, 1]$. In recent years, this model and its diluted version have
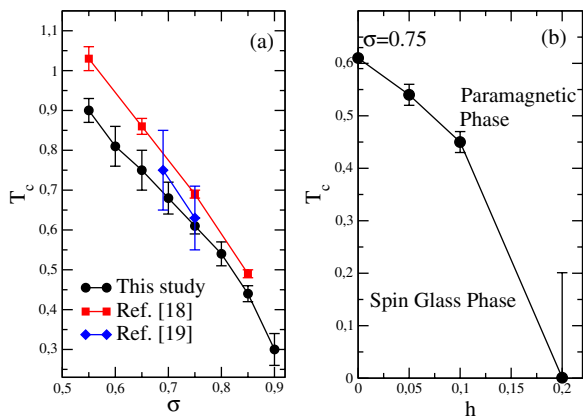
Fig. 5: (Color online) Panel (a): the critical temperatures of the power law one-dimensional Ising spin glass measured in refs. [26,27] and in this study are plotted for several values of σ in the absence of external field. Panel (b): the T-h phase diagram is reported for the same model with $\sigma = 0.75$.

been widely investigated in the literature [25–29], focusing on the identification of a transition in the presence of an external field, namely on the identification of the AT line. In these studies, T_c for different values of σ, both with and without the external field, has been measured with FSS analysis [25–29]. Contradictory results have been obtained in the non mean-field–like region in the presence of the external perturbation. When $h \neq 0$, indeed, Leuzzi et al. [28] find a finite critical temperature, whereas no transition has been observed by Katzgraber and Young [26,29].

We turn to consider our results. In all our simulations we consider systems with $N = 1024$ spins and final times up to 10000 Monte Carlo steps. We have explicitly checked that no finite-size effects are present. We first discuss results for different values of $\sigma \in [0.5, 0.9]$ without external field. In particular, in the left panels of figs. 3 and 4, we plot $X_2(\tau, T)$ for $\sigma = 0.55$, since $\theta_c = 1.09 \pm 0.02 > 1$, and $X(\tau, T)$ for $\sigma = 0.75$ vs. T for different τ. Curves clearly show intersection points, giving $T_c = 0.90 \pm 0.02$ and $T_c = 0.61 \pm 0.02$ for $\sigma = 0.55$ and for $\sigma = 0.75$, respectively. The critical temperature obtained from the same analysis for other values of σ are reported in the left panel of fig. 5, where previous results [26,27] are also shown. We find that T_c is a monotonously decreasing function of σ, consistent with a linear decay $T_C \sim 1 - 1.6(\sigma - 0.5)$, for $\sigma \in [0.5, 0.8]$, and a faster decay for larger σ. The monotonic decreasing behavior of T_c with increasing σ is expected, since larger values of σ correspond to shorter interaction ranges. Conversely, the results of ref. [26] show a decreasing linear behavior for $\sigma \geqslant 0.55$, but are expected to manifest a non-monotonic behavior approaching $\sigma = 0.5$, where the mean-field value $T_c = 1$ is imposed by eq. (5). We wish to notice that, for every choice of σ, we always obtain a value of T_c significantly smaller than the one obtained in ref. [26]. The value of T_c estimated in ref. [27] are intermediate between

our results and those of ref. [26], but due to the large error bar, are compatible with both findings.

Differences between the results of our method and those of ref. [26] become more pronounced when $h \neq 0$. More precisely, in the mean-field region, for $\sigma = 0.55$ and $h = 0.1$ we find $T_c = 0.71 \pm 0.03$, a value still smaller than that of ref. [26], $T_c = 0.96 \pm 0.02$. Conversely, an opposite trend is obtained in the non–mean-field region $\sigma > 2/3$, where we always find a $T_c > 0$, while no transition was obtained in ref. [26]. Let us stress that we can consider a uniform field $h_i = h$, whereas FSS analysis imposes the application of a spatially decorrelated (random) field.

In particular, we focus on $\sigma = 0.75$ and three values of h, $h = 0.05, 0.1, 0.2$. For $h = 0$ and $h = 0.1$, we consider longer simulations up to 50000 Monte Carlo steps and $N = 2048$ in order to avoid finite-size effects. Results for $X(T, \tau)$ are plotted in the main panels of fig. 4. The behavior of $T_c(\tau_i)$ vs. τ_i is plotted in the insets. Figures 4(b) and (c) show that curves intersect at a finite temperature indicating the existence of a phase transition in the presence of an external field. We notice that the curves spreading at low temperature is less pronounced than for smaller σ and other models. This can be attributed to the smaller value of θ_c. Indeed, from eq. (4), at fixed difference $\theta_c - \theta$ one has that $X_0 - X(\tau, T_c)$ is a decreasing function of θ_c. The measured values $T_c = 0.56 \pm 0.01$ and $T_c = 0.43 \pm 0.01$, for $h = 0.05$ and $h = 0.1$, respectively, are consistent with the expected trend of a decreasing T_c for increasing h. The inset of fig. 4(d) gives a non-constant $T_c(\tau_i)$ that decreases at small τ_i and tends to flatten only for the largest τ_i. The above trend suggests the absence of a finite T_c for $h = 0.02$ but does not exclude that $T_c(\tau_i)$ asymptotically converges to $T_c \in (0, 0.2)$ at large times. In the right panel of fig. 5 we plot the T-h phase diagram showing the existence of the AT line, separating the spin glass phase from the paramagnetic one.

In order to obtain more insights on the behavior of disordered systems, the same procedure can be carried out replacing $C(t)$ in eq. (2) by a multispin correlation function. Nevertheless, the non linear susceptibility $\chi_4(t, t_w) = \sum_{i,j} \langle s_i(t) s_j(t) s_i(t_w) s_j(t_w) \rangle$ usually considered in the investigation of disordered systems [14], is not properly suitable for this kind of study. Indeed, $\chi_4(t, t_w)$ encodes the typical length scale $L(t)$ of spatial correlation, and is expected to grow in time until a limit value that depends on $\xi(T)$ or $L(t_w)$ [30]. More precisely, for $L(t_w) < \xi(T)$, $X(\tau, T)$ would be not affected by $\xi(T)$ and, therefore, it would not be able to identify eventual divergences of $\xi(T)$. A way to overcome the above difficulty is to consider other multispin correlations, such as the second-order susceptibility considered in ref. [31]. This quantity is intimately related to $\chi_4(t, t_w)$ and converges to an asymptotic value controlled by $\xi(T)$, independently of t_w. This quantity can be used in the described procedure. Difficulties, in this case, are related to huge fluctuations of this second-order susceptibility that make the numerical evaluating very time-demanding.

In conclusion, we have introduced a dimensionless quantity $X(\tau, T)$ that is expected to become time independent at the critical temperature T_c. This allows one to identify T_c from the intersection of curves $X(\tau, T)$ for fixed τ and different T. The method has been tested in models where there exist accurate estimates of T_c, as the Ising ferromagnet and its diluted version. The study of the two-dimensional EA model confirms the absence of a transition at finite temperature. The method has been then applied to the one-dimensional Ising spin glass with power law decaying interactions for different choices of σ and h. Results for $h = 0$ give T_c values always smaller than those obtained by static FFS methods in ref. [26], with differences that are larger for smaller σ. In particular for $\sigma = 0.55$ we obtain $T_c = 0.90 \pm 0.02$, a value smaller than the one of ref. [26], where $T_c = 1.03 \pm 0.03$, unexpectedly above the mean-field value $T_c = 1$. The study in the presence of a finite perturbation $h > 0$ indicates the existence of a finite critical temperature also in the non–mean–field–like region $\sigma > 2/3$, in agreement with a replica symmetry breaking scenario.

$$* * *$$

REFERENCES

[1] Parisi G., *J. Phys. A*, **13** (1980) 1101.
[2] de Almeida J. R. L. and Thouless D. J., *J. Phys. A*, **11** (1978) 983.
[3] Fisher D. S. and Huse D. A., *Phys. Rev. B*, **38** (1988) 386.
[4] Barber M. N., in *Phase Transitions and Critical Phenomena*, edited by Comb C. and Lobowitz J. L., Vol. **8** (Academic Press, London) 1983.
[5] Nightingale M. P., *Physica A*, **83** (1975) 561.
[6] Ballesteros H. G., Fernández L. A., Martín-Mayor V. and Munoz Sudupe A., *Phys. Lett. B*, **378** (1996) 207; *Nucl. Phys. B*, **483** (1997) 707.
[7] Ballesteros H. G., Fernández L. A., Martín-Mayor V., Munoz Sudupe A., Parisi G. and Ruiz-Lorenzo J. J., *Phys. Rev. B*, **58** (1998) 2740.
[8] Luescher M., Weisz P. and Wolff U., *Nucl. Phys. B*, **359** (1991) 221.
[9] Palassini M. and Caracciolo S., *Phys. Rev. Lett.*, **82** (1999) 5128.
[10] Cooper F., Freedman B. and Preston D., *Nucl. Phys. B*, **210** (1982) 210.
[11] Janssen H. K., Schaub B. and Schmittmann B., *Z. Phys. B*, **73** (1989) 539; Zheng B., *Physica A*, **283** (2000) 80.
[12] Stauffer D., *Physica A*, **186** (1992) 197; Ito N., *Physica A*, **192** (1993) 604; Ozeki Y. and Ito N., *Phys. Rev. B*, **64** (2001) 024416.
[13] Bernardi L. W., Prakash S. and Campbell I. A., *Phys. Rev. Lett.*, **77** (1996) 2798; Pleimling M. and Campbell I. A., *Phys. Rev. B*, **72** (2005) 184429.
[14] Franz S., Donati C., Parisi G. and Glotzer S. C., *Philos. Mag. B*, **79** (1999) 1827.
[15] Blote H. W. J., Shchur L. N. and Talapov A. L., *Int. J. Mod. Phys. C*, **10** (1999) 1137.
[16] Huse D. A., *Phys. Rev. B*, **40** (1989) 304.
[17] Calabrese P. and Gambassi A., *Phys. Rev. E*, **65** (2002) 066120.
[18] Bray A., *Adv. Phys.*, **43** (1994) 357.
[19] Jaster A., Mainville J., Schulke L. and Zheng B., *J. Phys. A: Math. Gen.*, **32** (1999) 1395.
[20] McMillan W. L., *Phys. Rev. B*, **30** (1984) 476.
[21] Bray A. J. and Moore M. A., *J. Phys. C*, **17** (1984) L463; Bray A. J. and Moore M. A., in *Heidelberg Colloquium on Glassy Dynamics*, edited by van Hemmen J. L. and Morgenstern I. (Verlag, Springer) 1987.
[22] Hartmann A. K. and Young A. P., *Phys. Rev. B*, **64** (2001) 180404(R); Amoruso C., Marinari E., Martin O. C. and Pagnani A., *Phys. Rev. Lett.*, **91** (2003) 087201.
[23] Kotliar G., Anderson P. W. and Stein D. L., *Phys. Rev. B*, **27** (1983) R602; Moore M. A., *J. Phys. A: Math. Gen.*, **19** (1986) L211.
[24] Sherrington D. and Kirkpatrick S., *Phys. Rev. Lett.*, **35** (1975) 1792.
[25] Katzgraber H. G. and Young A. P., *Phys. Rev. B*, **67** (2003) 134410; **68** (2003) 224408.
[26] Katzgraber H. G. and Young A. P., *Phys. Rev. B*, **72** (2005) 184416.
[27] Leuzzi L., *J. Phys. A: Math. Gen.*, **32** (1999) 1417.
[28] Leuzzi L., Parisi G., Ricci-Tersenghi F. and Ruiz-Lorenzo J. J., *Phys. Rev. Lett.*, **101** (2008) 107203; **103** (2009) 267201.
[29] Katzgraber H. G., Larson D. and Young A. P., *Phys. Rev. Lett.*, **102** (2009) 177205.
[30] Corberi F., Lippiello E., Sarracino A. and Zannetti M., *J. Stat. Mech: Theory Exp.* (2010) P04003.
[31] Lippiello E., Corberi F., Sarracino A. and Zannetti M., *Phys. Rev. B*, **77** (2008) 021201; *Phys. Rev. E*, **78** (2008) 041120.